SUPPLEMENTARY METHODS

Generation of mice with *Aspm* deletion

ES cells containing a targeted allele of *Aspm* were obtained from the Knockout Mouse Project (KOMP) Repository (*Aspm*$^{Gt(KOMP)Wtsi}$; ES cell clone EPD0320_1_A06; here termed *Aspm*^{SA}). ES cells were injected into blastocysts to generate chimeras, which were crossed with albino C57 Bl6 mice. The resulting black mice were genotyped by PCR to identify mice heterozygous for insertion of a splice-acceptor cassette between exons 6 and 7 of *Aspm*. The selected *Aspm*$^{SA/+}$ mice were then back-crossed into C57 Bl6 mice, then intercrossed to generate *Aspm*$^{SA/SA}$, *Aspm*$^{SA/+}$, and *Aspm*$^{+/+}$ littermates.

Aspm is located on the forward strand of Chromosome 1E4. The targeting cassette contains a ~4500bp 5' homology arm spanning the intron between exons 3 and 4 and into exon 6, and a ~4700bp 3' homology arm spanning exon 7 to the intron between exons 9 and 10. This "knockout-first" targeted *Aspm*^{SA} allele inserts an FRT-flanked LacZ-neomycin (βgeo) cassette downstream of exon 6, and includes loxP sites flanking exon 7 (Fig. S2A). The βgeo cassette contains an *Engrailed2* splice acceptor that leads to aberrant splicing of exon 6 to the βgeo cassette, followed by stop codon and polyadenylation signal. This is predicted to produce an *Aspm* transcript truncated at nucleotide 2482 (corresponding to amino acid 774), subsequently fused to LacZ. A similar gene trap line was generated by the Sanger Institute Gene Trap Resource (SIGTR, *Aspm*$^{Gt(AA0137)Wtsi}$) and characterized by the Huttner lab, in which a βgeo cassette was inserted between exons 7 and 8, leading to truncation of *Aspm* at amino acid 794, which contains only the N-terminal microtubule domains and lacks the calponin homology domains and C-terminal calmodulin-binding isoleucine-glutamine (IQ) repeats (Pulvers et al., 2010). This gene-trap allele, *Aspm*$^{exons1-7}$, was shown to produce a truncated mRNA, and an antibody directed against the peptide region transcribed by exon3 of *Aspm* or against βgeo showed that a truncated protein was produced (Pulvers et al., 2010). This truncated protein was shown to localize to spindle poles at metaphase, though at reduced levels compared to wild-type Aspm; but was

absent from the midbody at telophase, in contrast to wild-type Aspm (Pulvers et al., 2010). Thus, it is likely that both *Aspm*$^{exons1-7}$ and our very similar *Aspm*^{SA} are hypomorphic alleles. In support of this, using qPCR primers specific to exons 24-25, we could not detect any full-length transcript in the homozygous *Aspm*$^{SA/SA}$ mutant (Fig. 3A), consistent with the fact that this transcript would be truncated at exon 6.

To generate a conditional allele of *Aspm* (*Aspm*$^{f/+}$, Fig. S2B), *Aspm*$^{SA/SA}$ mice were crossed with *Rosa26-FLPe* mice (Farley et al., 2000; strain 3946, Jackson Laboratories) . Mice were screened by PCR for the excision of the FRT-flanked splice-acceptor cassette and the presence of loxP sites flanking exon 7. *Aspm*$^{f/+}$ progeny were bred to wild-type C57 Bl6 mice, then bred to homozygosity of the *Aspm*$^{f/f}$ allele.

To conditionally delete *Aspm* in CGNPs, *Aspm*$^{f/f}$ and *Math1-cre* (Matei et al., 2005) lines were intercrossed, then back crossed with *Aspm*$^{f/f}$, generating the genotype *Math1-cre;Aspm*$^{f/f}$ (*Aspm* cKO). Deletion of exon 7 leads to introduction of a frameshift between exons 6 and 8. The N-terminal portion of the protein would be transcribed correctly through I774, but the frameshift is predicted to mutate G775D, followed by a short peptide, SFWRTDPSGRQQ, and a premature termination codon (Fig. S3C). This is likely to lead to nonsense mediated degradation of the truncated transcript, and in fact we detected minimal full-length *Aspm* transcript in the cKO cerebellum using RT-PCR primers spanning exons 24-25 (Fig. 3A). We interpret the residual *Aspm* full-length mRNA detected in *Aspm* cKOs (Fig. 3A) to be due to the fact that RNA was isolated from whole cerebella, and *Aspm* is only deleted in the Math1 lineage. Thus, *Aspm* mRNA present in blood vessels or other cell types in the cerebellum that express *Aspm* could account for the ~20% we detected in the cKOs compared to *Aspm*$^{f/f}$ controls.

To generate animals with *Aspm* deletion and medulloblastoma, *Aspm*$^{f/f}$ mice were crossed with *hGFAP-Cre* (Zhuo et al., 2001) and *SmoM2* (Mao et al., 2006) (Jackson Laboratories, strain 5130) mouse lines, and the resulting progeny were intercrossed to generate the genotypes *hGFAP-cre;SmoM2;Aspm*$^{f/f}$ (*G-Smo;Aspm*^{KO}) or *hGFAP-cre;SmoM2;Aspm*$^{f/+}$ (*G-Smo;Aspm*^{het}). *hGFAP-cre* mice express Cre during brain development in stem cells that give rise to diverse progeny, including the

entire cerebellum, excluding the Purkinje lineage (Zhuo et al., 2001; Kuang et al., 2012) and hGFAP-Cre;SmoM2 mice develop rapidly progressive medulloblastoma (Schüller et al., 2008).

PCR Primers and Primary Antibodies

For RT-qPCR: *Aspm* primers we used have been previously published (GCTTCATCACCTGCTCACCTAC and GTAGATACCGCTCCGCTTTCAG; Wu et al., 2008). Additional primer pairs were *CyclinD2* (GCGTGCAGAAGGACATCCA and CACTTTTGTTCCTCACAGACCTCTAG), *GAPDH* (TGTGTCCGTCGTGGATCTGA and CCTGCTTCACCACCTTCTTGA).

For genotyping: $Aspm^{SA}$ mice primers were TTGTATACAGCAGCTGTCCA, TACGAAGTTATGTCGAGATATCTAG, and TTGTGACATCAATATTCCTG, producing a ~300 bp band from the $Aspm^{SA}$ allele, and a ~400 bp band from the WT allele. $Aspm^{fl}$ primers were TTGTATACAGCAGCTGTCCA and TTGTGACATCAATATTCCTG, producing a ~500 bp band from the floxed allele and a ~400 bp band from the WT allele. Math1-cre primers were GCGGTCTGGCAGTAAAAACTATC and GTGAAACAGCATTGCTGTCACTT, producing a ~200 bp band. SmoM2 primers were AAGTTCATCTGCACCACCG and TCCTTGAAGAAGATGGTGCG, producing a ~200 bp band.

Primary antibodies (all except as noted from Cell Signaling, Danvers, MA, USA): cC3 (cat#9661), PCNA (cat#2586), Survivin (cat#2808), pHH3 (cat#9706), γ□□□□ (cat#9718), BrdU (Accurate Scientific, Westbury NY, cat#OBT0030G), Ki67 (Leica Biosystems/Novocastra, cat#NCL-L-Ki67-MM1), and p27 (Dako, Carpinteria, CA, cat#M7203).

Quantitative analysis of mitotic progression, spindle orientation, BrdU/p27, cC3, γH2AX and tumor cross sectional area

For analyses of proliferation, cerebellar sections were imaged on a 4-channel Leica DM5500 confocal SPEII microscope using LAS acquisition software to perform high magnification (32x) tilescans with a 20x ACS Apochromat 20x/0.60 multi-immersion objective. For images of mitotic cells, an ACS

Apochromat 63x/1.30 oil objective was used to perform z-stacks that confirmed division orientation. Mitotic stages were identified by the combination of Survivin and pHH3 staining patterns (Fig. 4G), and were manually counted using the cell counting module in LAS software. Two independent mid-sagittal sections from 3-4 animals of each genotype were analyzed, typically including 200-400 mitotic cells/section. Due to breeding schemes for *Aspm;Bax* double mutant analyses, *Aspm*$^{f/+}$*;Bax*$^{f/+}$*;Math1-Cre* mice were used as controls, as their cell cycle profile was indistinguishable from *Aspm*$^{f/f}$ wild-type mice (compare blue bars in Fig. 4H and Fig. 7H). Mitotic cell counts were normalized to EGL area to control for differences in cerebellum size between controls and *Aspm* cKOs, and because individual cells in the EGL were too densely-packed to accurately count. EGL and IGL area were determined with ImageJ, using a thresholded binary image of the DAPI channel. The position of each mitotic cell was determined by measuring its distance from the pial surface and dividing this value by the width of the EGL at that position (Fig. S3A). Values of <0.5 were considered EGL_S, and >0.5 EGL_D, which corresponded well with both morphologic differences in cell shape between cells in the oEGL and iEGL, as well as the boundary between PCNA and p27 expression at these ages (P5-P7, see Figs 3K-M).

For anaphase metrics, the shape of daughter pronuclei was analyzed using ImageJ to determine the aspect ratio (AR), where a value of 1.0 corresponds to a circle and higher values indicate more elliptical shapes. Z-stacks were taken to confirm that only cells dividing within the plane of imaging were quantified, thus avoiding potential error in measurements due to oblique angle divisions. The distance between daughter pronuclei (d) was measured between centromeres using ImageJ. Division orientation was determined for both anaphase and telophase cells as shown in Fig. 5A. Perpendicular divisions were defined as those in which the angle bisecting the daughter pronuclei and the pial membrane was greater than 45°, and parallel were less than 45°. Transverse divisions were defined as those in which Survivin staining was evident, generally in a semi-circular pattern, but only one daughter pronucleus could be visualized beneath it. This orientation was confirmed through z-stacks, and ambiguous cells were excluded from the analyses. Data were collected and exported from ImageJ into Microsoft Excel, then binned, analyzed, and plotted using GraphPad Prism.

For BrdU incorporation, P5 littermate pups were injected with 50 mg/kg BrdU and sacrificed 24 or 48 hours later. Mid-sagittal brain sections were double labeled with antibodies to BrdU (Accurate Scientific, Westbury NY, cat#OBT0030G) and p27 (Dako, Carpinteria, CA, cat#M7203). For the 48 hour pulse, the fraction of p27+ cells in the iEGL, molecular layer (ML) and IGL that were BrdU+ was quantified using Metamorph's multiwavelength cell scoring module (Fig. 5M). For the 48 hour pulse, analysis included 5 (control) or 7 (*Aspm* cKO) sections from 3 (control) or 4 (*Aspm* cKO) littermates; for the 24 hour pulse, 4 sections (1 from each littermate animal) were analyzed for each genotype. Typically 3000-5000 BrdU+ cells per section were present and counted in each region. BrdU+ cells which were p27+ and p27- were manually counted and scored for the data presented in Figs 5L,N,O,P.

To quantify cC3+, TUNEL and γ□□□□ positive cells in the cerebellum, nuclei were counterstained with hematoxylin or DAPI, slides were digitized on an Aperio Scanscope and analyzed using Aperio Software (Aperio, Vista, CA, USA) for chromogen-stained slides or Tissue Studio (Definiens, München, Germany) for fluorescence. The entire EGL region was manually annotated and used for quantifications, which were normalized to the total number of nucleated cells in the designated region. Positive cells were manually counted and classified as EGL_S or EGL_D based on their position within the EGL (< or > 50% of EGL depth, respectively). To control for differences in cerebellum size between genotypes, counts were normalized to EGL length, quantified by manually tracing the outer perimeter of the cerebellum in ImageJ.

In Figure 3, to quantify the area of the EGL and IGL, we used ImageJ to threshold the DAPI channel, and manually defined the region of interest (ROI) to be restricted to the EGL or IGL, respectively (Fig. 3J). For calculations of the PCNA+ area of the EGL (oEGL) and p27+ area of the EGL (iEGL) in Figs 3M,N, similar procedures were used to threshold the PCNA and p27 channels. The perimeter (length) of the EGL was traced and calculated in ImageJ, and oEGL/PCNA+ and iEGL/p27+ thickness was determined by dividing these areas by the EGL length (Fig. 3N). EGL perimeter was similarly used to normalize counts of apoptotic cells in Fig. 5L and Fig. 6D. In Figs 4C,D,F and Figs 7F,G, similar procedures were used to calculate EGL area, whereby the DAPI channel was used to generate a binary threshold image, whose area was calculated in ImageJ. This area measurement was

used to normalize counts of mitotic cells, given the differences in EGL area between genotypes, where *Aspm* cKOs showed a ~20% reduction on average.

To compare tumor size between the *G-Smo;Aspm*^{KO} and *G-Smo;Aspm*^{het} genotypes, brains sections were stained with H&E and the sections with the maximum cross-sectional diameter were selected. In these sections, tumor was identified by hypercellular pathology, nuclear shape, and intense hematoxylin staining. Normal cerebellum was identified by histologic features, including cellularity and nuclear shape within in the relatively hypercellular IGL. Tumor and non-tumor areas were annotated manually and measured using Aperio software. Tumor area was normalized to the area of normal cerebellum in order to consider proportion of total cerebellum attributable to tumor.

Volumetric MRI studies

For volumetric MRI studies, P30 mice were perfused and brains were dissected free and fixed for 48 hours in 4% formaldehyde in PBS. Brains were then washed in PBS and then transferred to Fomblin Y04 solution (Kurt J. Lesker Company, Cat#:MFY06/6BB) 24 hours before scanning. Brains were then imaged in pairs on a Bruker Biospec 9.4T horizontal bore scanner with a RARE 3D sequence using TR = 3000 ms, TEeff = 60 ms, RARE factor = 8, field of view = 4.2x1.4x1 cm, matrix size = 420x140x100, resulting in 100µm isotropic resolution. Whole brain volume was quantified using Amira software (FEI Visualization Sciences Group, Bordeaux, France) with intraventricular space excluded after tissue segmentation. For cerebellar measurements, images were analyzed using ITK-SNAP software (www.itksnap.org) (Yushkevich et al., 2006). 3D scans were projected as sets of linked slices in the sagittal, coronal and axial orientations and the cerebellar region was manually annotated in each slice. The cerebellar volume was thus defined and measured within the software environment. Measured volumes were grouped by genotype and the two-tailed students' t-test was used to compare volumes between genotypes.

Supplementary Figures

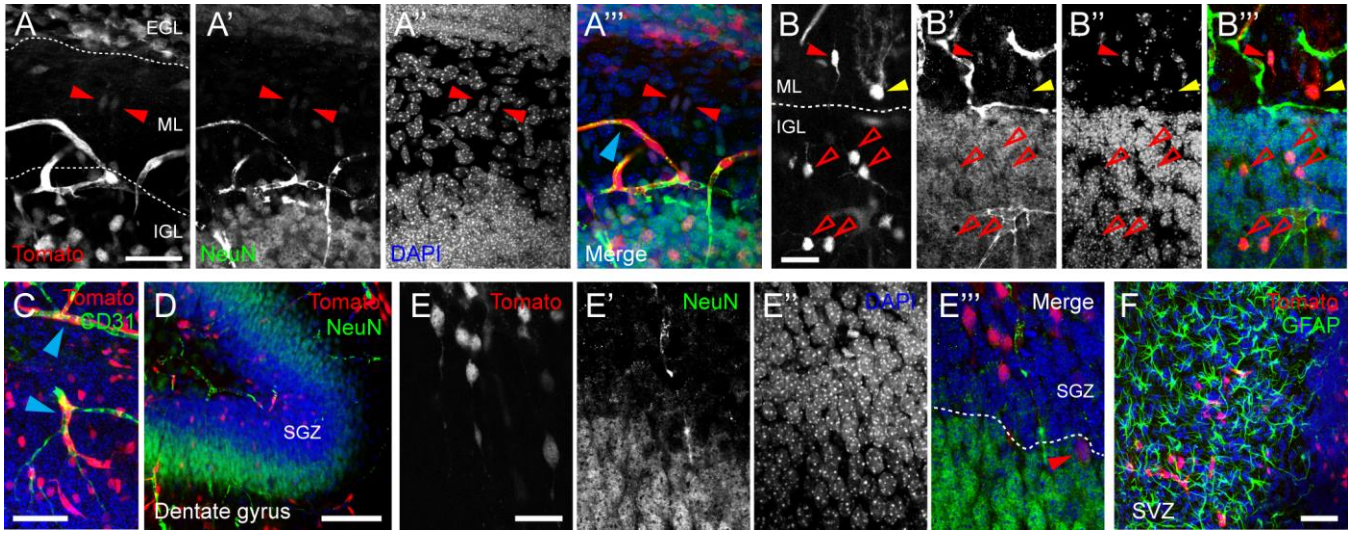

Supplementary Figure 1. Fate of *Aspm-CreER;Rosa26-TdTomato* descendants in cerebellum and hippocampus.
A-A''') Confocal section of P7 cerebellum pulsed with tamoxifen at P4. Red arrowheads indicate migrating GNs in the molecular layer (ML). Note also TdTomato+/NeuN+ GNs in the IGL. **B-B'''**) Confocal section of P7 cerebellum stained as in (**A**) showing TdTomato+/NeuN+ GNs in the IGL (hollow red arrowheads) and migrating GN in the ML (solid red arrowhead). A TdTomato+ interneuron in the plexiform layer that is weakly NeuN+, likely a Lugaro cell, is indicated by the yellow arrowhead. **C)** TdTomato+/CD31+ endothelial cells in P11 cerebellum, indicating that Aspm is also expressed in blood vessels. **D,E)** Confocal sections of P7 dentate gyrus (DG) region of the hippocampus following a 3 day pulse with tamoxifen at low (**D**) and high (**E**) magnification. Progenitors reside in the NeuN- subgranular zone (SGZ) and show the characteristic bipolar radial glia-like morphology. One example of a differentiated TdTomato+/NeuN+ hippocampal DG neuron is indicated by the red arrowhead in (**E'''**). **F)** Aspm-derived progenitors in the subventricular zone (SVZ) of the P11 cerebral cortex are not of glial (GFAP+) origin. Scale bars: 50 µm in (**A,C,E**); 25 µm in (**B**); 100 µm in (**D**).

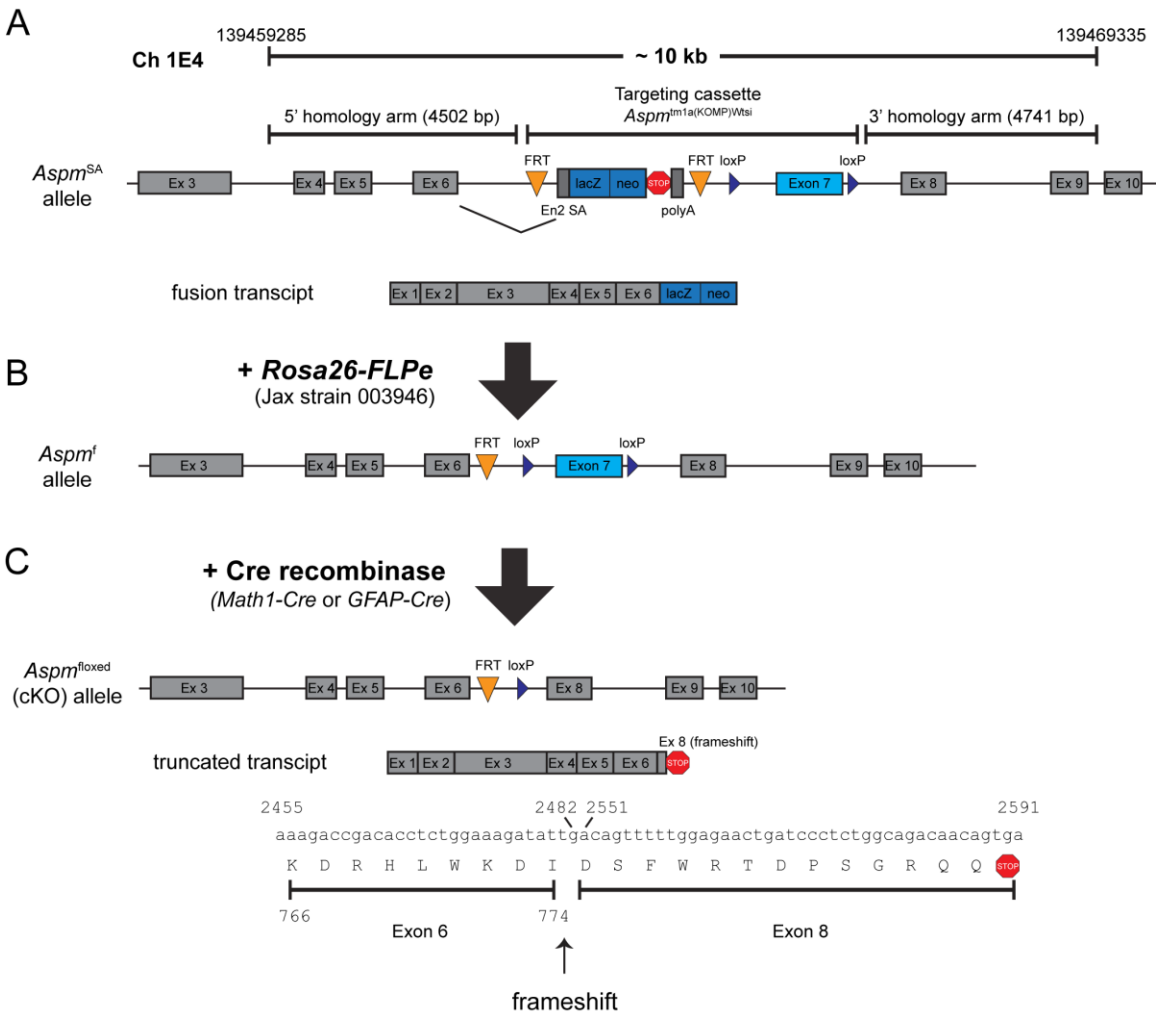

Supplementary Figure 2. Description of *Aspm* targeting vectors and mutant alleles.
A) Diagram of *Aspm* gene locus on chromosome 1E4, with targeting vector used to create the "knockout first" *Aspm*^{SA} allele shown (See Supplemental Methods for details). This targeting vector inserts an FRT-flanked LacZ-neomycin (βgeo) cassette downstream of exon 6, and includes loxP sites flanking exon 7. The predicted protein product of this insertion is a fusion of exon 6 to the βgeo cassette via the *Engrailed2* splice acceptor. **B)** The *Aspm*^{SA} allele can be reverted to a wild-type allele by excision of the FRT-flanked βgeo cassette using flipase. This was accomplished by mating with the *Rosa26-FLPe* line, expressing the enhanced FLP recombinase under expression of the ubiquitous Rosa26 promoter. The resultant line *Aspm*^{f} retains loxP sites in the introns surrounding exon 7 but produces a wild-type transcript. **C)** The *Aspm*^{f} allele can then be converted to a conditional predicted null by crossing with transgenic lines expressing Cre recombinase in a tissue-specific manner. Deletion of exon 7 is predicted to introduce a frameshift that leads to a premature stop codon early in exon 8. To generate CGNP conditional cKOs, we used the *Math1-Cre* line, while the *hGFAP-Cre* line was used for medulloblastoma models.

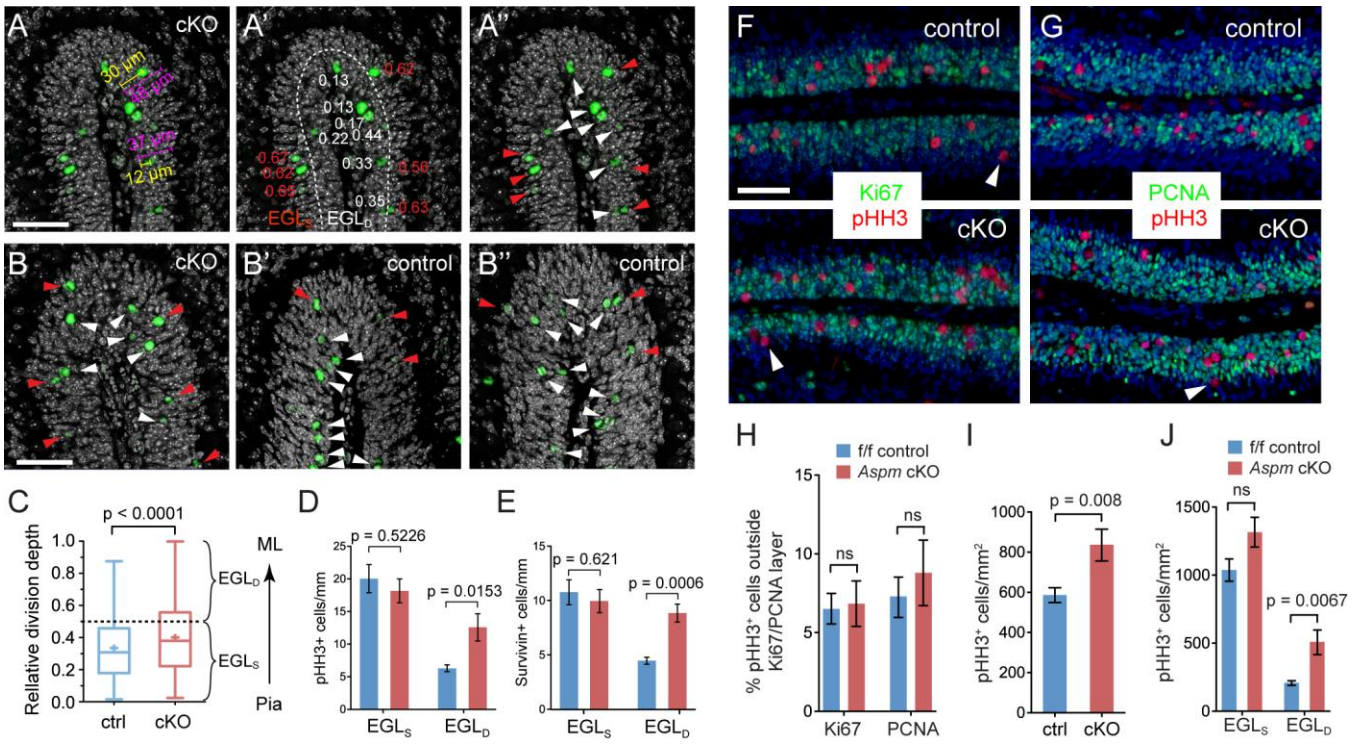

Supplementary Figure 3. Distribution of proliferating cells in the EGL in *Aspm* cKOs. **A,B)** Representative regions of cerebellum between lobes III and IV labeled for pHH3 (green) and DAPI (gray). **A)** The depth of pHH3+ cells is calculated by measuring the distance from the pia (yellow) and dividing by the thickness of the EGL (magenta), shown here for two cells. **A'**) Depth measurements for all pHH3+ cells in this section, as quantified using the metric in (**A**). The approximate boundary between the EGL_S and EGL_D is shown by the dotted line, equivalent to half the distance between the pia and boundary of the EGL and molecular layer. Cells located within the EGL_S are labeled in white and those within the EGL_D in red. **A'')** White arrowheads indicate cells within the EGL_S and red arrowheads, those within the EGL_D. **B-B'')** Additional cKO (**B**) and *Aspm*$^{f/f}$ control (**B',B''**) sections indicating position of mitotic cells within the EGL_S (white arrowheads) and EGL_D (red arrowheads), as in (**A''**). Note increase in pHH3+ figures within the EGL_D in *Aspm* cKOs. **C)** Box-and-whisker plots of the position of mitotic cells in control and *Aspm* cKOs, showing a tendency toward deeper divisions in the cKO. **D,E)** Quantification of mitotic cell density by pHH3 (**D**) and Survivin (**E**) staining in the EGL_S and EGL_D, normalized to EGL length. **F,G)** Representative regions of lobe VII for P7 *Aspm*$^{f/f}$ control and *Aspm* cKO cerebellum labeled with pHH3 and Ki67 (**F**) or PCNA (**G**) to label cycling cells in the oEGL. White arrowheads indicate rare mitotic cells located outside of the Ki67/PCNA zone. **H)** Quantification of the frequency in which pHH3+ cells are found outside of the Ki67 or PCNA zone, showing no significant difference between controls and *Aspm* cKOs. Note that even pHH3+ outliers are also positive for Ki67 or PCNA. **I,J)** In this data cohort, the frequency of mitotic cells was analyzed and again found to be higher in cKOs (compare Fig. S3I to Fig. 4C). The increased incidence of mitotic figures was located mainly in the EGL_D (compare Fig. S3J to Fig. 4F). Scale bars: 50 µm.

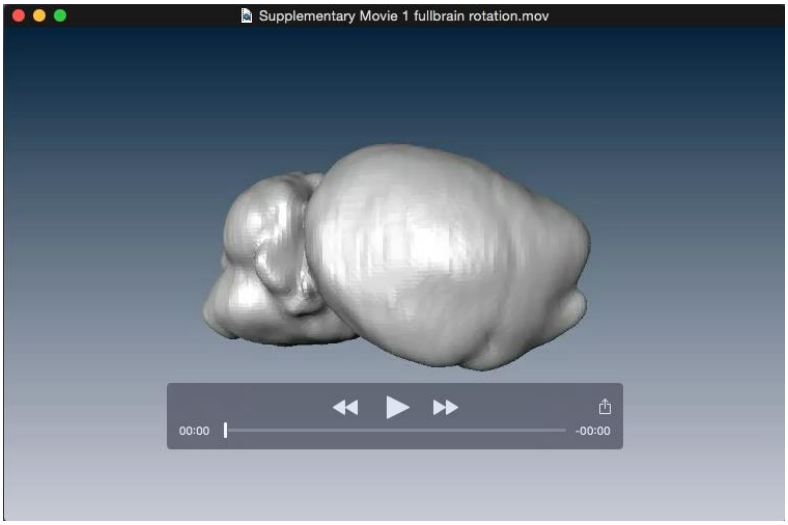

Supplementary Movies 1 and 2. Representative animated, rotating 3-dimensional MRIs of the mouse brain and digitally isolated cerebellum, obtained from an $Aspm^{SA/SA}$ mouse.

Video clip shows the whole brain (1) or cerebellar region (2), rotated to reveal all sides.